Correlation radiometer and calibration theory.

Rob Streeter, Gabriel Santamaria Botello,
Kaitlin Hall, Zoya Popović

August 26, 2021

1 Definitions

Consider the radiometer of Fig. 1. Each device (hybrid couplers, amplifiers, etc) has waveguides connected to their ports, through which traveling electromagnetic fields $\boldsymbol{E}(\boldsymbol{r},t) = a(t)\boldsymbol{E}_0(\boldsymbol{r})$ and $\boldsymbol{H}(\boldsymbol{r},t) = a(t)\boldsymbol{H}_0(\boldsymbol{r})$ propagate. Here, $a(t)$ is a random process associated with a thermal source, and in a strict sense, should have a broadband blackbody spectrum. However, since the pre-detection filters in Fig. 1 determine the narrowband portion of the spectrum that is relevant for the following analysis, we treat $a(t)$ as a band-limited process centered at ν_0 (for the prototype presented in this paper, $\nu_0 = 1.412\,\mathrm{GHz}$). As such, it can always be expressed as a slow-varying complex amplitude $x(t)$ modulating a tone:

$$
\begin{aligned}
a_k(t) &= \frac{\sqrt{2}}{2} x_k(t) e^{i2\pi\nu_0 t} + \text{c.c.} \\
&= \sqrt{2}\,\mathrm{Re}\{x_k(t)\}\cos(2\pi\nu_0 t) \\
&- \sqrt{2}\,\mathrm{Im}\{x_k(t)\}\sin(2\pi\nu_0 t),
\end{aligned}
\tag{1}
$$

where the sub-indices $k = 1,\ldots,5$ specify a given signal in Fig. 1. Signals $x_k(t)$ (and thus, $y_{1,2}(t)$) are zero-mean Gaussian-distributed complex random processes, with a spectrum that follows the normalized shape of the pre-detection

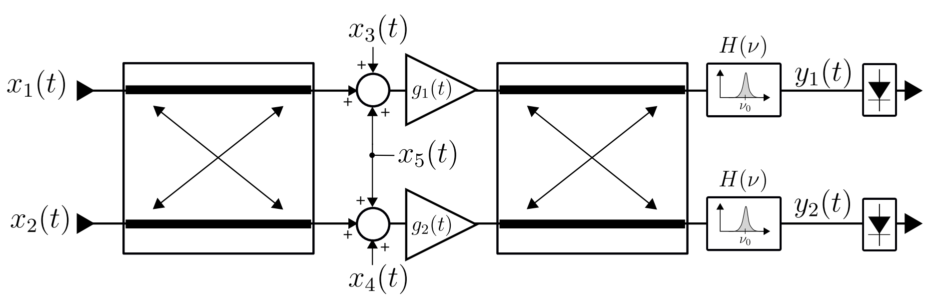

Figure 1: Scheme of correlation radiometer.

filters $H(\nu)$, where $H(\nu_0) = 1$. This implies the couplers and amplifiers' spectral responses are approximately flat within the bandwidth of $H(\nu)$.

The modal fields $\boldsymbol{E}_0(\boldsymbol{r})$, $\boldsymbol{H}_0(\boldsymbol{r})$ are normalized such that $\int_{S_T} \boldsymbol{E}_0(\boldsymbol{r}) \times \boldsymbol{H}_0(\boldsymbol{r})\, \mathrm{d}S = 1$, where S_T is the waveguide's cross section, so the cycle-averaged instantaneous power results

$$P_k(t) = \nu_0 \int_{t-\nu_0^{-1}}^{t} \int_{S_T} \boldsymbol{E}(\boldsymbol{r}, t) \times \boldsymbol{H}(\boldsymbol{r}, t)\, \mathrm{d}S\, \mathrm{d}t \tag{2}$$

$$= \nu_0 \int_{t-\nu_0^{-1}}^{t} a_k^2(t)\, \mathrm{d}t = |x_k(t)|^2. \tag{3}$$

The processes $\mathrm{Re}\{x_k(t)\}$ and $\mathrm{Im}\{x_k(t)\}$ are uncorrelated [1] and each has the same power spectral density $S_{x_k x_k}(\nu)/2$, determined by the filter $H(\nu)$ shifted to baseband[1]: $H_0(\nu) = H(\nu+\nu_0)\mu(\nu+\nu_0)$, where $\mu(\nu)$ is the Heaviside function, i.e.,

$$S_{x_k x_k}(\nu) = \frac{\langle P_k(t) \rangle}{\Delta\nu} H_0(\nu), \tag{4}$$

where $\Delta\nu$ is the power-equivalent bandwidth:

$$\Delta\nu = \int_0^\infty H(\nu)\, \mathrm{d}\nu = \int_{-\infty}^\infty H_0(\nu)\, \mathrm{d}\nu. \tag{5}$$

2 Noise sources

The amplifiers add input-referred uncorrelated zero-mean Gaussian noise $x_{3,4}(t)$ with total power $\left\langle |x_{3,4}(t)|^2 \right\rangle = k_B T_{3,4} \Delta\nu$ and a power spectral density following the shape of $H_0(\nu)$. The couplers are lossy and thus add noise since they have non-zero physical temperature T_{phys}. The noise added by the output coupler is negligible because it is located after the high gain amplification stage.

Assuming a perfectly matched and isolated lossy coupler, its S-parameter matrix takes the form

$$S = \begin{bmatrix} 0 & S_{12} & S_{13} & 0 \\ S_{12} & 0 & 0 & S_{24} \\ S_{13} & 0 & 0 & S_{34} \\ 0 & S_{24} & S_{34} & 0 \end{bmatrix}. \tag{6}$$

Incident and reflected waves at each port can be arranged in column vectors $\boldsymbol{a}$ and $\boldsymbol{b}$ respectively. Then, $\boldsymbol{b} = \boldsymbol{S}\boldsymbol{a} + \boldsymbol{n}$, where $\boldsymbol{n}$ is a vector of thermal noise sources with power spectral density determined by $H_0(\nu)$. The degree of correlation of the elements of $\boldsymbol{n}$ can be found from the generalized Nyquist theorem for multiport networks [2] as

[1] We are assuming the response of the radiometer is linear up to the signals $y_{1,2}(t)$, hence the filter is accounted for as it were right behind the inputs of the radiometer.

$$
\begin{aligned}
\langle \boldsymbol{n}\boldsymbol{n}^{\dagger} \rangle &= \begin{bmatrix} \langle n_1 n_1^* \rangle & \langle n_1 n_2^* \rangle & \langle n_1 n_3^* \rangle & \langle n_1 n_4^* \rangle \\ \langle n_2 n_1^* \rangle & \langle n_2 n_2^* \rangle & \langle n_2 n_3^* \rangle & \langle n_2 n_4^* \rangle \\ \langle n_3 n_1^* \rangle & \langle n_3 n_2^* \rangle & \langle n_3 n_3^* \rangle & \langle n_3 n_4^* \rangle \\ \langle n_4 n_1^* \rangle & \langle n_4 n_2^* \rangle & \langle n_4 n_3^* \rangle & \langle n_4 n_4^* \rangle \end{bmatrix} \qquad (7) \\
&= \left(I - SS^{\dagger}\right) k_B T_{\text{phys}} \Delta\nu, \qquad (8)
\end{aligned}
$$

where the dagger indicates Hermitian conjugate and I is the identity matrix. The noise budget of the radiometer is influenced by the thermal noise leaving ports 2 and 3 of the coupler: $n_2(t)$ and $n_3(t)$ respectively. Inserting Eq. (6) into Eq. (8), we obtain their power and correlation:

$$
\begin{aligned}
\langle n_2(t) n_2^*(t) \rangle &= \left(1 - |S_{24}|^2 - |S_{12}|^2\right) k_B T_{\text{phys}} \Delta\nu \qquad (9) \\
\langle n_3(t) n_3^*(t) \rangle &= \left(1 - |S_{34}|^2 - |S_{13}|^2\right) k_B T_{\text{phys}} \Delta\nu \qquad (10) \\
\langle n_2(t) n_3^*(t) \rangle &= \left(-S_{12} S_{13}^* - S_{24} S_{34}^*\right) k_B T_{\text{phys}} \Delta\nu. \qquad (11)
\end{aligned}
$$

We can split each noise source into uncorrelated and correlated parts, i.e.,

$$
\begin{aligned}
n_2(t) &= n_2'(t) + x_5(t) \qquad (12) \\
n_3(t) &= n_3'(t) + x_5(t), \qquad (13)
\end{aligned}
$$

such that $\langle n_2'(t) n_3'^*(t) \rangle = \left\langle n_{2,3}'(t) x_5^*(t) \right\rangle = 0$, and thus

$$
\begin{aligned}
\left\langle \left|n_{2,3}(t)\right|^2 \right\rangle &= \left\langle \left|n_{2,3}'(t)\right|^2 \right\rangle + \left\langle \left|x_5(t)\right|^2 \right\rangle \\
&= k_B (T_{2,3}' + T_5) \Delta\nu,
\end{aligned} \qquad (14)
$$

$$
\langle n_2(t) n_3^*(t) \rangle = \left\langle \left|x_5(t)\right|^2 \right\rangle = k_B T_5 \Delta\nu. \qquad (15)
$$

The power of processes $n_{2,3}'(t)$ and $x_5(t)$ can be obtained from eqs. (15) and (14) by inserting the coupler's response into eqs. (9)–(11). Sources $n_2'(t)$ and $n_3'(t)$ can be included into $x_3(t)$ and $x_4(t)$ by adding powers as they are uncorrelated processes. Process $x_5(t)$ adds to the input of each amplifier. For the input coupler used in the experiments, we estimate $T_2' \approx 16.4\,\text{K}$, $T_3' \approx 13.5\,\text{K}$ and $T_5 \approx 3.8\,\text{K}$ at $T_{\text{phys}} = 290\,\text{K}$. The temperature of the noise added by each amplifier is about $43\,\text{K}$.

3 Input/Output relations

Assuming the couplers and amplifiers response is flat within $\Delta\nu$, and the group delay of the radiometer is much lower than $\Delta\nu^{-1}$, the measurement outputs

$y_{1,2}(t)$ are simply linear combinations of the inputs $x_{0,\ldots,5}(t)$ evaluated at the same instant[2] t:

$$y_i(t) = \sum_{k=1}^{5} a_{ik}(t) x_k(t), \quad i = 1, 2 \tag{16}$$

Equation (16) is the general case. In the following and for illustration purposes, we find the coefficients a_{ik} resulting from particular assumptions.

3.1 Ideal case

Assuming ideal couplers, we have $S_{12} = 1/\sqrt{2}$, $S_{24} = -i/\sqrt{2}$, $S_{13} = -i/\sqrt{2}$, $S_{34} = 1/\sqrt{2}$. According to Fig. 1, the output of identical amplifiers with field gain g, is

$$b_1(t) = g\left(\frac{1}{\sqrt{2}} x_1(t) - i\frac{1}{\sqrt{2}} x_2(t) + x_3(t) + x_5(t)\right) \tag{17}$$

in the upper branch, and

$$b_2(t) = g\left(-i\frac{1}{\sqrt{2}} x_1(t) + \frac{1}{\sqrt{2}} x_2(t) + x_4(t) + x_5(t)\right) \tag{18}$$

in the lower branch. After $b_{1,2}(t)$ are superimposed in the output coupler, we get

$$\begin{aligned} y_1(t) &= -igx_2(t) + \frac{g}{\sqrt{2}}\left[x_3(t) - ix_4(t) + (1-i)x_5(t)\right] \\ y_2(t) &= -igx_1(t) - \frac{g}{\sqrt{2}}\left[ix_3(t) - x_4(t) - (1-i)x_5(t)\right]. \end{aligned} \tag{19}$$

Comparing Eq. (19) with Eq. (16), we obtain the coefficients summarized in the first two columns of Table 1.

3.2 Effect of gain fluctuations

We can describe the field gain of the amplifiers $g_1(t) = g(1 + \alpha_1(t))$ and $g_2(t) = g(1 + \alpha_2(t))$ as being Gaussian complex random processes with mean $g + \langle\alpha_1\rangle$ and $g + \langle\alpha_2\rangle$ respectively, and power spectral density proportional to $\nu^{-\beta/4}$. Here, $\beta \approx 1$, such that the power gain has a $\propto 1/\nu^\beta$ noise power spectrum. Following a similar procedure to that of previous section, we obtain the coefficients summarized in the last two columns of Table 1.

[2] If the group delay is not comparatively short, a rigorous notation should include such group delay.

a_{ij}	Ideal		With gain fluctuations	
$j \backslash i$	1	2	1	2
1	0	$-ig$	$\frac{g}{2}\left(\alpha_1-\alpha_2\right)$	$-ig\left(1+\frac{\alpha_1+\alpha_2}{2}\right)$
2	$-ig$	0	$-ig\left(1+\frac{\alpha_1+\alpha_2}{2}\right)$	$\frac{g}{2}\left(\alpha_2-\alpha_1\right)$
3	$\frac{g}{\sqrt{2}}$	$-i\frac{g}{\sqrt{2}}$	$\frac{g}{\sqrt{2}}(1+\alpha_1)$	$-i\frac{g}{\sqrt{2}}(1+\alpha_1)$
4	$-i\frac{g}{\sqrt{2}}$	$\frac{g}{\sqrt{2}}$	$-i\frac{g}{\sqrt{2}}(1+\alpha_2)$	$\frac{g}{\sqrt{2}}(1+\alpha_2)$
5	$\frac{1-i}{\sqrt{2}}g$	$\frac{1-i}{\sqrt{2}}g$	$\frac{g}{\sqrt{2}}\left(1-i+\alpha_1-i\alpha_2\right)$	$\frac{g}{\sqrt{2}}\left(1-i+\alpha_2-i\alpha_1\right)$

Table 1: Values of a_{ij} for ideal amplifiers and amplifiers having gain fluctuations $\alpha_1(t)$, and $\alpha_2(t)$.

3.3 Moments and correlations

The cycle-averaged power measured at each output of the radiometer is

$$Q_i(t) = y_i(t)y_i^*(t) = \sum_{j=1}^{5}\sum_{k=1}^{5} a_{ij}(t)a_{ik}^*(t)x_j(t)x_k^*(t). \tag{20}$$

Taking the expected value of Eq. (20), we can factorize the processes $x(t)$ from the processes $a(t)$ since gain fluctuations and thermal noise sources are statistically independent, i.e.,

$$\langle Q_i(t)\rangle = \sum_{j=1}^{5}\sum_{k=1}^{5} \langle a_{ij}(t)a_{ik}^*(t)\rangle \langle x_j(t)x_k^*(t)\rangle . \tag{21}$$

The term $\langle x_j(t)x_k^*(t)\rangle = \langle P_j\rangle \delta_{jk}$, where δ_{jk} is the Kronecker delta and $\langle P_j\rangle = k_B T_j \Delta\nu$ the mean power of the process $x_j(t)$. To show this, we expand each process into real and imaginary parts $x_n(t) = x_{nr}(t) + ix_{ni}(t)$:

$$\begin{aligned}\langle x_j(t)x_k^*(t)\rangle &= \langle x_{jr}(t)x_{kr}(t)\rangle \\ &\quad + i\,\langle [x_{ji}(t)x_{kr}(t) - x_{jr}(t)x_{ki}(t)] + x_{ji}(t)x_{ki}(t)\rangle .\end{aligned} \tag{22}$$

The imaginary part of Eq. (22) vanishes when taking the expected value because real and imaginary parts of different or the same process are uncorrelated [1], and also have zero mean. The real part of Eq. (22) vanishes unless $j = k$, in which case equals $\left\langle |x_j(t)|^2 \right\rangle = \langle P_j\rangle$. Therefore,

$$\langle Q_i(t)\rangle = \sum_{j=1}^{5} \left\langle |a_{ij}(t)|^2 \right\rangle \langle P_j\rangle . \tag{23}$$

Equation (23) implies the mean power measured by each detector is a linear combination of the individual noise source mean powers. Hence, provided the detectors are working in the square-law region, their mean output voltages $\langle V_i(t)\rangle$ are linear combinations of the individual noise source temperatures T_j, i.e.,

$$\langle V_i(t)\rangle = R_i k_B \Delta\nu \sum_{j=1}^{5} \left\langle |a_{ij}(t)|^2 \right\rangle T_j, \tag{24}$$

where R_i (V/W) is the responsivity of the detector i. In the ideal case,

$$\begin{aligned} \langle V_1(t)\rangle &= R_1 k_B \Delta\nu |g|^2 \left(T_2 + \frac{T_3 + T_4}{2} + T_5 \right) \\ \langle V_2(t)\rangle &= R_2 k_B \Delta\nu |g|^2 \left(T_1 + \frac{T_3 + T_4}{2} + T_5 \right). \end{aligned} \tag{25}$$

Therefore, if the two detectors are identical ($R_1 = R_2 = R$), then $\langle V_2(t)\rangle - \langle V_1(t)\rangle \propto T_1 - T_2$, and the knowledge of the proportionality constant (radiometer gain) and the reference temperature T_2 is sufficient to retrieve the unknown temperature T_1, regardless of the internally generated noise.

4 Calibration

Owing to imbalances in the couplers, amplifier gains, and detector responsivities, Eq. (24) does not perfectly reduce to Eq. (25). Instead, we must expect the mean output voltage at each detector to be a full unique linear combination of $T_{1,\ldots,5}$. As show next, we can characterize the radiometer by performing a static measurement with three different known pairs of input temperatures T_1 and T_2 (three-point calibration). This way, the dependence of the radiometer on $T_{1,2}$ is known, with an accuracy limited by radiometric noise or gain fluctuations, depending on the integration time τ.

From Eq. (24), we can express the two mean output voltages $\langle V_1\rangle = \alpha_{11}T_1 + \alpha_{12}T_2 + \alpha_{13}$ and $\langle V_2\rangle = \alpha_{21}T_1 + \alpha_{22}T_2 + \alpha_{23}$, where $\alpha_{jk},\ j,k = 1,2,3$ are constants, neglecting the effects of gain fluctuations. The contributions of the internal noise sources (functions of $T_{3,4,5}$) are all included in the offset terms α_{13} and α_{23}. Such terms might also include any offset voltage introduced by imperfect post-detection amplifiers. Clearly, α_{13} and α_{23} depend strongly on the ambient temperature. However, as the radiometer approximates to the ideal one, $\alpha_{13} \to \alpha_{23}$ for any ambient temperature. Therefore, the effects of ambient temperature are mitigated by taking the difference between both voltages, just as it would be done in the ideal case:

$$\begin{aligned} \langle \Delta V(t)\rangle &= \langle V_2(t)\rangle - \langle V_1(t)\rangle \\ &= \underbrace{(\alpha_{21} - \alpha_{11})}_{\Delta_1} T_1 + \underbrace{(\alpha_{22} - \alpha_{12})}_{\Delta_2} T_2 + \underbrace{\alpha_{13} - \alpha_{23}}_{\Delta_3}. \end{aligned} \tag{26}$$

Then, if $\Delta_{1,2,3}$ and T_2 are known, the probe's temperature is estimated from the measured voltage difference $\overline{\Delta V(t)} = \overline{V_2(t)} - \overline{V_1(t)}$, averaged over some time τ:

$$T_1^{\mathrm{estim}} = \frac{\overline{\Delta V(t)} - \Delta_2 T_2 - \Delta_3}{\Delta_1}. \tag{27}$$

To find $\Delta_{1,2,3}$, we test the radiometer with three different pairs of known input temperatures $(T_1^{(i)}, T_2^{(i)}),\ i = 1, 2, 3$ and measure the three differential outputs $\overline{\Delta V(t)}^{(i)}$. Then, the system

$$\underbrace{\begin{bmatrix} \overline{\Delta V(t)}^{(1)} \\ \overline{\Delta V(t)}^{(2)} \\ \overline{\Delta V(t)}^{(3)} \end{bmatrix}}_{b} = \underbrace{\begin{bmatrix} T_1^{(1)} & T_2^{(1)} & 1 \\ T_1^{(2)} & T_2^{(2)} & 1 \\ T_1^{(3)} & T_2^{(3)} & 1 \end{bmatrix}}_{A} \underbrace{\begin{bmatrix} \Delta_1 \\ \Delta_2 \\ \Delta_3 \end{bmatrix}}_{x} \tag{28}$$

is solved for the vector x containing $\Delta_{1,2,3}$. The accuracy of the solution depends on the condition number of the matrix A, which is improved with the geometrical distance between temperature points (pairs of input temperature values).

5 Temperature resolution considerations

5.1 Effects of antenna mismatch and efficiency on system noise

Suppose a scene at temperature T_A is observed with an antenna having a mismatch coefficient Γ and a radiation efficiency η. The antenna is connected to a radiometer with system temperature T_{sys} and total chain gain G. Thus, the output power P_0 measured in a narrow bandwidth determined at the backend is

$$\langle P_0 \rangle = KG \left[T_{\mathrm{sys}} + \eta \left(1 - |\Gamma|^2 \right) T_A + (1 - \eta) T_{\mathrm{phys}} \right], \tag{29}$$

where T_{phys} is the physical (room) temperature of the antenna, and K a constant incorporating the bandwidth and Boltzmann constant. The scene temperature is estimated by averaging the output power during some interval τ, $\overline{P_0}$, removing the internal noise offset and scaling, i.e.:

$$T_A^{(\mathrm{est})} = \frac{1}{\eta \left(1 - |\Gamma|^2 \right)} \left[\frac{\overline{P_0}}{KG} - T_{\mathrm{sys}} - (1 - \eta) T_{\mathrm{phys}} \right], \tag{30}$$

where the offset level and scaling required is obtained from calibration. The uncertainty in the estimation ΔT_A is therefore proportional to the uncertainty in the sample-averaged output power ΔP_0, being $\eta^{-1} \left(1 - |\Gamma|^2 \right)^{-1} K^{-1} G^{-1}$ the porportionality constant. Since P_0 arises from the superposition of different thermal sources, it follows the radiometer equation

$$\Delta P_0 = K_{\text{arch}} \frac{\langle P_0 \rangle}{\sqrt{B\tau}}, \tag{31}$$

where B is the noise equivalent bandwidth, and K_{arch} a constant on the order of unity that depends on the radiometer architecture. Inserting Eq. (29) into Eq. (31), we get

$$\Delta T_A = K_{\text{arch}} \frac{1}{\sqrt{B\tau}} \left[\frac{T_{\text{sys}}}{\eta \left(1 - |\Gamma|^2\right)} + T_A + \frac{(1-\eta) T_{\text{phys}}}{\eta \left(1 - |\Gamma|^2\right)} \right]. \tag{32}$$

Therefore, the effect of an antenna mismatch and non-ideal radiation efficiency, is the degradation of the original system noise temperature by a factor $K_{\text{deg}} = \eta^{-1} \left(1 - |\Gamma|^2\right)^{-1}$, and the addition of a noise temperature $T_{\text{add}} = K_{\text{deg}}(1 - \eta) T_{\text{phys}}$.

5.2 Comparison between architectures

The total power radiometer presents the highest temperature resolution (lowest uncertainty) that can be achieved with any conceivable classical device that measures the power of thermal radiation [3, 4]. That uncertainty is determined by the classical radiometer equation

$$\Delta T_A = \frac{T_A + T_{\text{sys}}}{\sqrt{B\tau}}, \tag{33}$$

where T_{sys} accounts for all noise sources in the apparatus. However, the total power radiometer cannot correct for gain fluctuations in the amplifiers, so other architectures such as e.g., Dicke switching or correlation are commonly used. In a Dicke radiometer, a frontend switch alternates the detection between the desired scene and a reference matched load at a known physical temperature. The switching has to be faster than the expected gain fluctuations. Then, the difference between the observations at each switch state is taken. The uncertainty of the observation at each state follows the same total-power radiometer equation, assuming reference load and antenna temperatures match. Since both observations are statistically independent, taking the difference increases the total uncertainty by a factor $\sqrt{2}$. As each observation is performed during half of the total cycle observation period τ, an additional factor $\sqrt{2}$ must be included. Finally, the total uncertainty in a Dicke radiometer is $K_{\text{arch}} = 2$ times that of the total-power radiometer equation.

In contrast, in a correlation radiometer both observations are done simultaneously for which the effective integration time is not halved. However, the difference between the power measured at each branch is taken, so a factor $K_{\text{arch}} = \sqrt{2}$ must be included to the total-power radiometer equation to find the uncertainty in the correlation radiometer. This means the temperature resolution is $\sqrt{2}$ times better in a correlation radiometer is than in a Dicke radiometer.

References

[1] B. Oliver, "Thermal and quantum noise," *Proceedings of the IEEE*, vol. 53, no. 5, pp. 436–454, 1965.

[2] H. Haus, *Electromagnetic Noise and Quantum Optical Measurements*, ser. Advanced Texts in Physics. Springer Berlin Heidelberg, 2000. [Online]. Available: https://books.google.com/books?id=qxaEVZXXNM8C

[3] J. Zmuidzinas, "Thermal noise and correlations in photon detection," *Appl. Opt.*, vol. 42, no. 25, pp. 4989–5008, Sep 2003. [Online]. Available: http://ao.osa.org/abstract.cfm?URI=ao-42-25-4989

[4] G. Santamaría-Botello, Z. Popovic, K. A. Abdalmalak, D. Segovia-Vargas, E. R. Brown, and L. E. García Muñoz, "Sensitivity and noise in thz electro-optic upconversion radiometers," *Scientific Reports*, vol. 10, no. 1, p. 9403, Jun 2020. [Online]. Available: https://doi.org/10.1038/s41598-020-65987-x